ADVANCED PHYSIOLOGICAL MONITORING OF FCS SOLDIERS

L. M. Hively* **and V. A. Protopopescu**
Oak Ridge National Laboratory
Oak Ridge, TN 37831-6418

ABSTRACT

We quantify dynamical change in nonlinear time-serial data via dissimilarity measures between statistical distribution functions. These new measures are superior to traditional nonlinear measures, and give robust and timely forewarning of normal-to-abnormal transitions in physiological regimes. These novel measures also provide rapid quantitative assessment of physiological change, such as alertness, soldier readiness, and bioagent exposure.

1. INTRODUCTION

Characterization of change in complex system dynamics is particularly difficult for physiological processes, which share several confounding features: non-stationarity, nonlinearity, multiple time scales, and strong sensitivity to environmental perturbations. The process dynamics can be quantified by traditional nonlinear measures, such as: (i) the first minimum, M_1, in the mutual information function, which is a measure of nonlinear de-correlation time; (ii) the correlation dimension, D, which quantifies dynamical complexity; and (iii) the Kolmogorov entropy, K, which is an indicator of predictability (or equivalently, the rate of nonlinear information loss). Kolmogorov entropy and correlation dimension are usually defined in the limit of zero scale length. However, all real data have noise and even noiseless model data are limited by the finite precision of computer arithmetic. Finite-scale values of K and D do not capture the full dynamical complexity of these processes in the absence of noise and have smaller values than expected for the zero-scale-length limit. In general, traditional nonlinear measures can distinguish between clear-cut regular and chaotic dynamics. However, they are not sufficiently sensitive to discern between *slightly different* chaotic regimes, especially when data are limited and/or noisy. This lack of discrimination arises from averaging over the global dynamics, which erases most of the dynamical details.

We address these limitations in traditional nonlinear measures via new measures to quantify change in time-serial data (including machines) as follows. We convert time-serial data to a discrete geometric (phase space) representation. A distribution function describes the visitation frequency and sequence of the discrete phase-space states; (un)changing dynamics lead to an (un)altered distribution function. Dissimilarity measures quantify the distance between a test case distribution function and the baseline distribution function. Large dissimilarity means that the system is far from the baseline, as a forewarning of an abnormal event, particularly in human data. A comparison of the results shows a significant and consistent superiority of our new measures over traditional nonlinear measures for detection and forewarning of condition change in real physiological data.

We organize the paper as follows. Section 2 discusses the analysis methodology and our new dissimilarity measures. Section 3 presents the results, as applied to physiological time series. We summarize the conclusions in Section 4, with acknowledgments in Sect. 5.

2. ANALYSIS METHODOLOGY

We begin with a process-indicative scalar signal, e, that is sampled at equal time intervals, τ, starting at time t_0, yielding a time series $e_i = e(t_0 + i\tau)$, $i = 1, 2, \ldots, N$. Physiologic data are usually affected by artifacts (e.g., eye blinks, muscle twitches). We remove essentially all of these artifacts by fitting a parabola to e_i over a moving window of $2w+1$ points with the same number of data points, w, on either side of a central point. We use the fitted value at the central point to estimate the artifact signal, f_i. Subsequent analysis uses only the artifact-filtered data, $x_i = e_i - f_i$, which is essentially artifact-free.

We extract the main features of the underlying dynamics via a dynamical reconstruction technique. Specifically, we form a d-dimensional time-delay vector, $y(i) = [x_i, x_{i+\lambda}, \ldots, x_{i+(d-1)\lambda}]$. The choice of lag, λ, and embedding dimension, d, determine whether the data are under-sampled (projected upon themselves) or redundant. This phase-space approach is used for both our new measures of condition change and the traditional nonlinear measures; see the reference for more details. We also note that different system observables contain dissimilar information. Thus, phase-space reconstruction can be easier from one variable, but more difficult (or even impossible) from another. Our analysis seeks a balance between these caveats and the practical constraint of a limited amount of noisy data.

Sensitive change discrimination uses the phase-space reconstruction of the reconstructed dynamics, as follows. We first represent each continuous value, x_i, as a discrete symbol, s_i, that is one of S different integers, 0, 1, …, S–1:

$$0 \le s_i = INT[S(x_i - x_{min})/(x_{max} - x_{min})] \le S - 1. \qquad (1)$$

The function, *INT*, converts a decimal number to the closest lower integer. The minimum and maximum values of x_i are x_{min} and x_{max}, respectively, over the baseline (reference data). We require that $s_i(x_i = x_{max}) = S - 1$ in order to maintain exactly S distinct symbols. The discretized vector, $y(i) = [s_i, s_{i+\lambda}, \ldots, s_{i+(d-1)\lambda}]$, partitions the phase space into S^d hypercubes or bins. We count the number of phase-space points in each bin to obtain a distribution function. We denote the population of the i-th bin of the distribution function as Q_i for the baseline, and R_i for a test case. The parameters (S, N, d, and λ) depend on the specific data, and reflect the underlying dynamics.

We compare the distribution functions of the test case and baseline dynamics by measuring the difference between Q_i with R_i by the χ^2 statistics and L_1 distance:

$$\chi^2 = \sum_i (Q_i - R_i)^2/(Q_i + R_i), \qquad (2)$$

$$L = \sum_i |Q_i - R_i|. \qquad (3)$$

The sums in Eq. (2 - 3) run over all of the populated phase-space cells. These measures account for changes in the geometry and occurrence frequency of the distribution function. The sum in the denominator of Eq. (2) is based on a test for equality of two multinomial distributions.

3. APPLICATION TO PHYSIOLOGICAL DATA

We present five illustrations of our approach by comparing traditional nonlinear measures (D and K) with phase-space dissimilarity measures (χ^2 and L). Direct comparison of these measures is difficult due to their disparate range, variability, and physical meaning. Renormalization allows meaningful comparison by defining V_i as the value of each indicator for the i-th cutset from the set, $V = \{D, K, \chi^2, \text{ and } L\}$. We denote the mean value of that indicator over the base case by $\underline{V}$, with a corresponding sample standard deviation, σ. A renormalized indicator is then $U(V) = |V_i - \underline{V}|/\sigma$, which measures the number of standard deviations that the test case deviates from the baseline mean. Dynamical states close to (far from) the baseline have small (large) values of the renormalized dissimilarity.

1. Human electroencephalogram data were acquired during clinical epilepsy monitoring and analyzed by the procedure of Section 2. Figure 1 shows typical results. Raw data in subplot (a) have very complex, non-periodic features that are typical of brain waves. The seizure event occurred at 110.7 minutes, as denoted by the solid vertical line in subplots (d) and (e). No seizure event forewarning is provided by the correlation dimension in subplot (b), or by the Kolmogorov entropy in subplot (c). The isolated peaks at 42 and 58 minutes in subplot (c) are not significant. An event forewarning of 27 minutes is provided by $U(\chi^2)$ in subplot (d) and $U(L)$ in subplot (e), with two (or more) successive occurrences above the threshold of 5 (dashed horizontal line) at 85 minutes (vertical dashed line). Hively and Protopopescu (2003) give additional details on the methodology for this and subsequent examples.

2. Human electrocardiogram data were acquired during ambulatory monitoring. Figure 2 shows results for a ventricular fibrillation event at 37 minutes. The raw data in subplot (a) show ten distinct heartbeats and their associated quasi-periodic (nonlinear) features. The correlation dimension in subplot (b) varies randomly (no forewarning features) with a rise at the fibrillation event. The Kolmogorov entropy in subplot (c) varies erratically; the peaks occurring at 8 and 24 minutes are not valid forewarning indications. Event forewarning of 16 minutes (the vertical dashed line) is provided by both $U(\chi^2)$ in subplot (d) and $U(L)$ in subplot (e); forewarning corresponds to two (or more) successive occurrences above the threshold (dashed horizontal line). Similar results were obtained for several additional datasets.

3. Human electrocardiogram data were acquired during laboratory tests of fainting (syncope), under the following protocol: (i) lying horizontal for 10 minutes, (ii) lying in tilted condition (70° from horizontal) for 40 minutes, and (iii) lying horizontal again for 5 minutes. Figure 3 (top) shows non-syncopal results with low values of renormalized dissimilarity (~10) that increase very slowly and erratically over the tilt period (slope, A~0.06-0.07 per minute). Figure 3 (bottom) shows syncopal results for the same subject with much larger renormalized dissimilarity (40-70) that increase much more rapidly over the tilt period (A~0.8-1 per minute). The tilt period in this second test was terminated early when the subject fainted. Similar results are obtained for a second subject.

4. Heart wave data were obtained via surface chest electrodes from anesthetized rats subjected to an induced sepsis experiment. After 55 minutes of normal-state recording, each test rat was exposed to inhaled bacterial endotoxin that induces an inflammatory response and eventually sepsis. Figure 4 shows sample results. Raw data in subplot (a) have distinct heartbeats with additional quasi-periodic (nonlinear) features. No indication of condition change is displayed by either the correlation dimension in subplot (b), or by the Kolmogorov entropy in subplot (c). The condition change is shown clearly by both $U(\chi^2)$ in subplot (d) and $U(L)$ in subplot (e), which

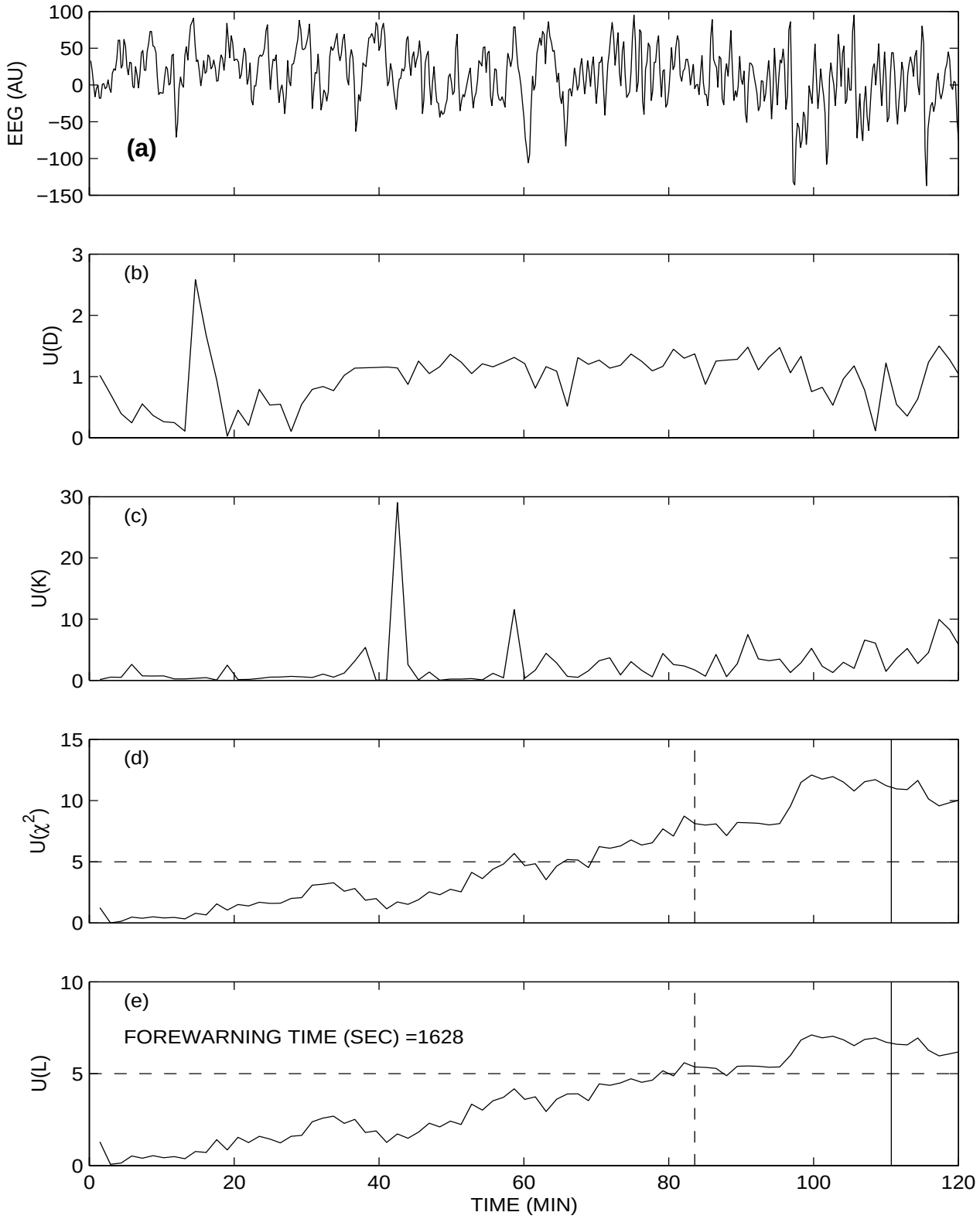

Figure 1: Results for human electroencephalogram channel 5 of dataset #PVM006, showing time-serial plots for: (a) 2.4 seconds of raw data collected at 250Hz, (b) correlation dimension, D, (c) Kolmogorov entropy, K, (d) $U(\chi^2)$, and (e) $U(L)$. The phase-space dissimilarity measures in subplots (d) and (e) are for $d = 3$, $S = 20$, $\lambda = 17$, and after removal of eye blink artifacts. Each cutest has $N = 22{,}000$ points, corresponding to 88 seconds. We have successfully applied this analysis to over sixty human datasets

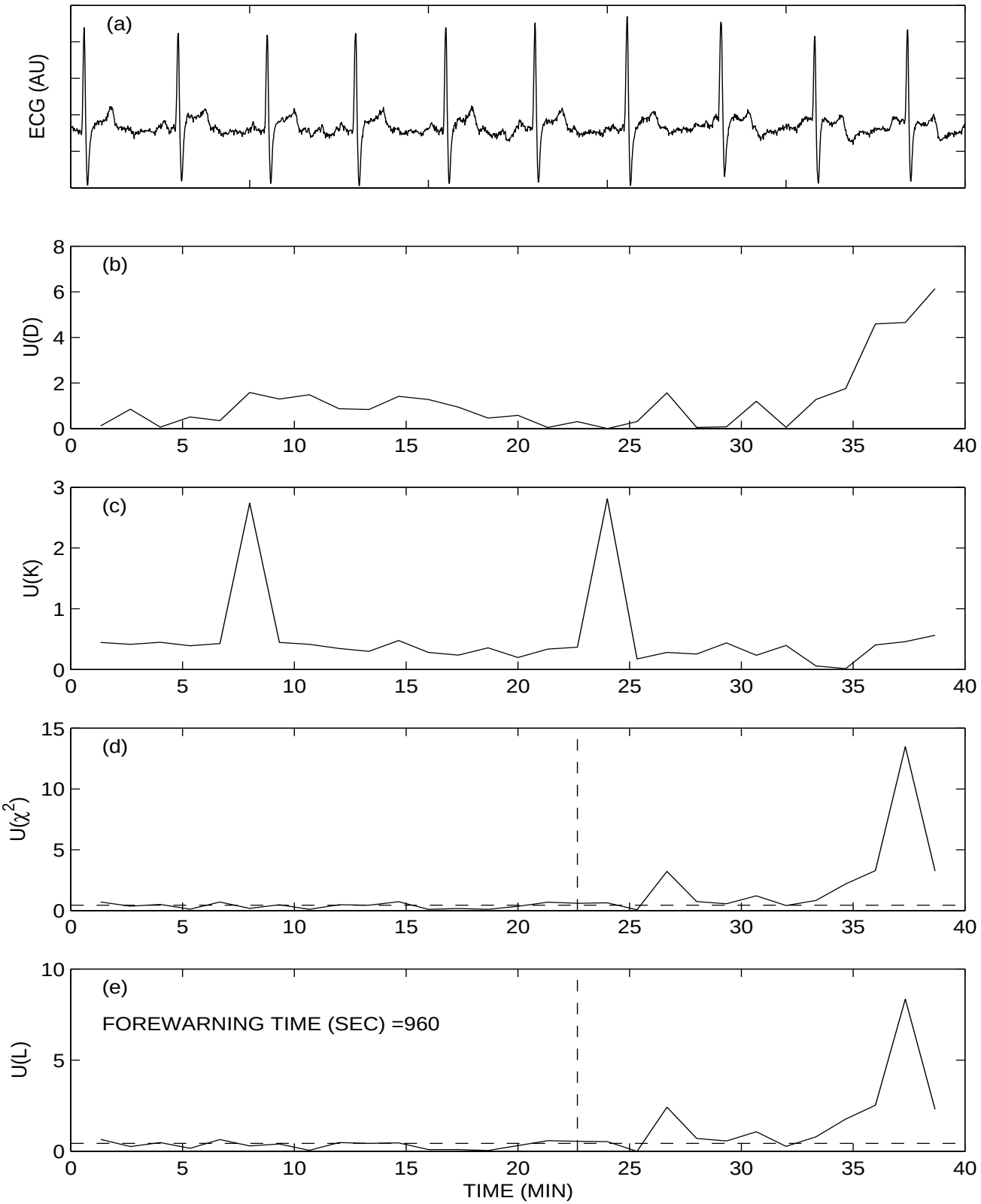

Figure 2: Results for human dataset #EC8202, showing time-serial plots for: (a) 10 seconds of raw heart wave data collected at 250 Hz, (b) correlation dimension, D, (c) Kolmogorov entropy, K, (d) $U(\chi^2)$, and (e) $U(L)$. The phase-space dissimilarity measures in subplots (d) and (e) are for d= 5, S = 3, λ = 27, after removal of breathing artifacts. Each cutest had N = 18,000 points, corresponding to 72 seconds.

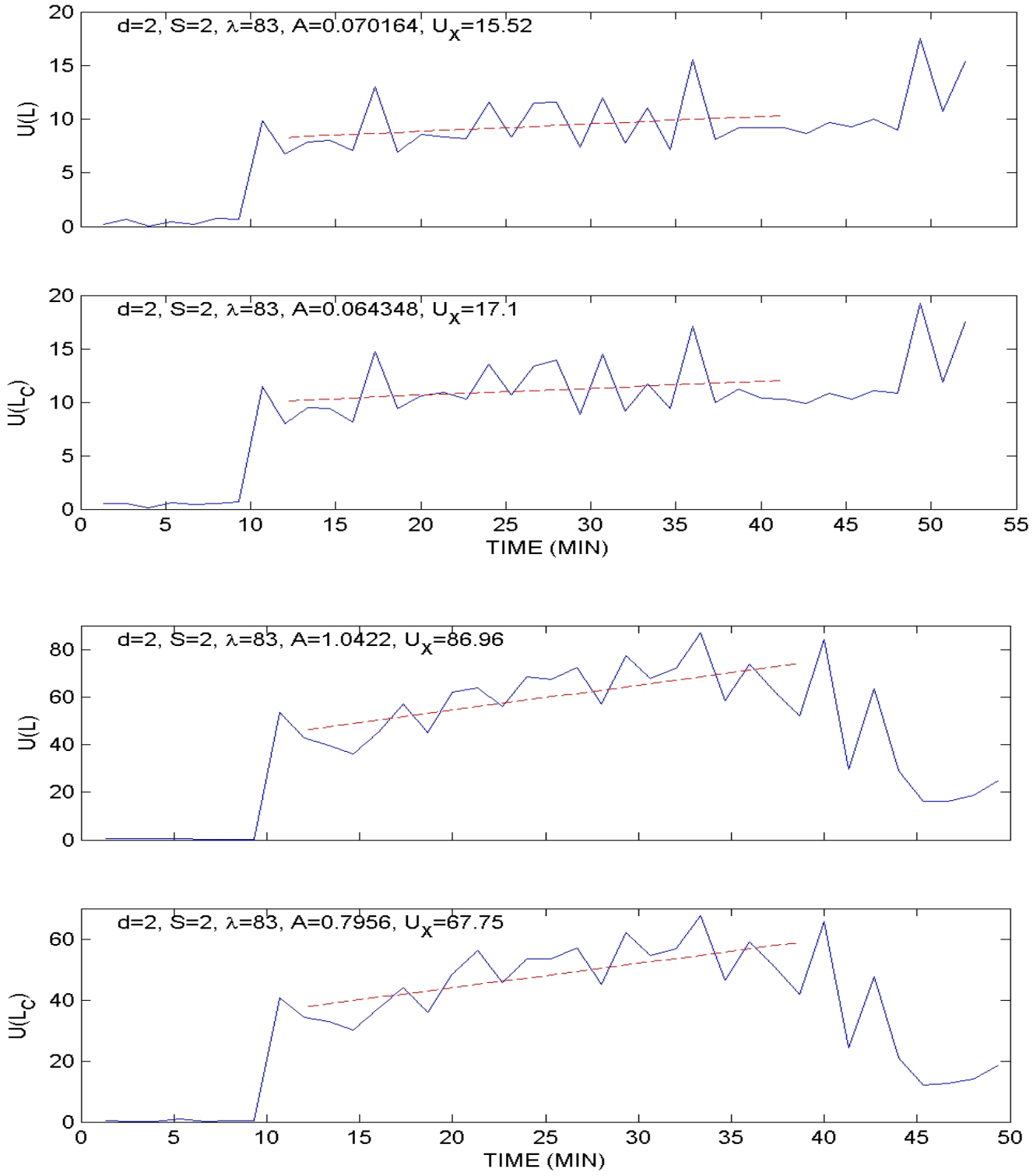

Figure 3: Results for human subject RAY show $U(L)$ and $U(L_C)$ when no syncope occurs (above the double line), in contrast with $U(L)$ and $U(L_C)$ when syncope does occur (below the double line). No results for traditional nonlinear measures are shown, due to their insensitivity in the other examples. The phase-space dissimilarity measures are for d =2, S = 2, λ = 83, after removal of breathing artifacts. Each cutest has N=20,000 points (80 seconds of data at a sampling rate of 250 Hz).

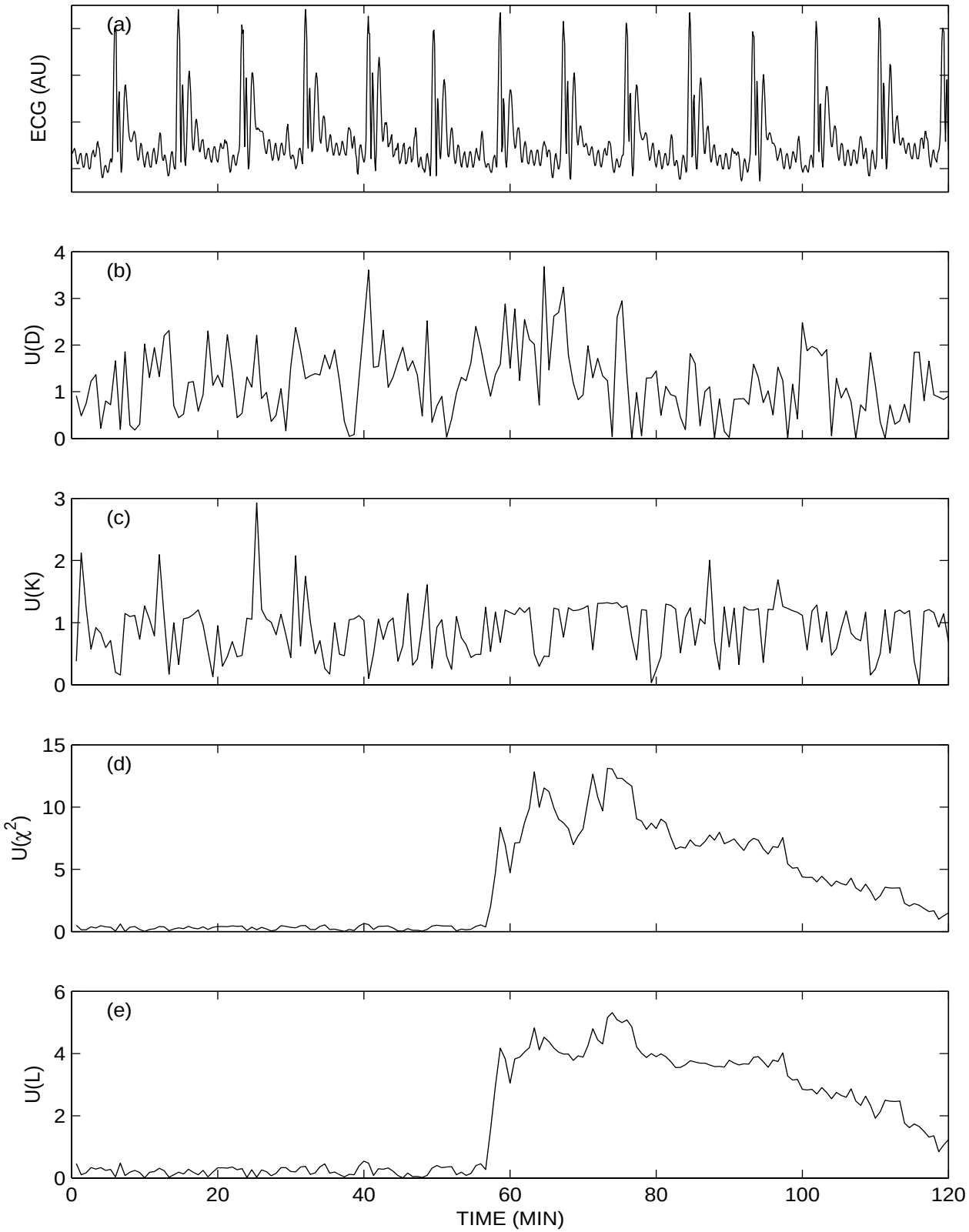

Figure 4: Results for dataset #33209V, showing time-serial plots for: (a) 2.4 seconds of raw rat heart wave data collected at 500 Hz, (b) correlation dimension, *D*, (c) Kolmogorov entropy *K, (d)* $U(\chi^2)$, and (e) $U(L)$. The phase-space dissimilarity measures in subplots (d) and (e) are for d =2, S = 2, λ = 80, after removal of breathing artifacts. Each cutest has N=20,000 points (40 seconds of data).

remains low for the first 57 minutes, rising abruptly after the exposure onset, remaining high for the next 20 minutes, then decreasing slowly as the immune response fought off the bioagent effects. This recovery response is consistent with other physiological observations during the test (not shown). The total true (negative) positive rate for (un)exposed animals is (6/6) 17/17.

5. A surface stethoscope acquired lung sounds data during lung experiments on anesthetized pigs. The baseline state consisted of normal breathing. Subsequent test cases were obtained by injecting a controlled volume of air (in increments of 100 milliliters up to 1400 milliliters) in the space between the diaphragm and the lungs, making breathing increasingly more difficult. Figure 5 shows sample pneumothorax results. Raw lung sounds data in subplot (a) have very complex features, including quasi-periodic heartbeats that are superimposed on breath-cycle undulations. The correlation dimension in subplot (b) provides no clear indication of condition change. The Kolmogorov entropy in subplot (c) likewise varies erratically. Condition change is indicated by both $U(\chi^2)$ in subplot (d) and $U(L)$ in subplot (e); both rise to a plateau of 5 over 100-500 ml, then increase to values larger than 20 over 500-1300 ml thereby providing robust forewarning of the animal's death at 1400 ml. Similar results were obtained for a second animal.

4. CONCLUSIONS

We have developed a model-independent method for measuring physiological condition change. First, we remove confounding artifacts (such as eye-blinks and breathing) with a novel zero-phase quadratic filter. The artifact-filtered data are converted into a statistical distribution function that describes the visitation frequency and sequence of the dynamical states. Dissimilarity measures between baseline and test data detect the change by summing the absolute values of the differences between distribution functions. The methodology is quite general and applies to a variety of physiological data, as shown by five examples: (1) brain waves for forewarning of epileptic events (Fig. 1); (2) heart waves for forewarning of ventricular fibrillation (Fig. 2), and for detection of syncope (Fig. 3) and sepsis (Fig. 4); and (3) lung sounds for detection of breathing difficulty (Fig. 5). The dissimilarity measures have small values in the normal state, followed by significantly larger values above a "normality threshold," indicating abnormal dynamics. The results show that the phase-space dissimilarity approach is sensitive, robust, and timely.

Our new approach also detects dynamical change in various physical processes. Examples include: detecting balanced and unbalanced centrifugal pump conditions from motor power; distinguishing different drilling conditions from spindle motor current of a machining center; and predicting failure of a bellows coupling in a rotating drive train from motor current; discerning the difference in micro-cantilever vibrations with and without mercury on the sensor; forewarning of failure in electrical motors; and forewarning of failure in motor-driven components.

We now have high-fidelity laboratory integration of the technology elements into desktop-computer software that analyzes noisy, archival data and provides change indication. The analysis is much faster than real-time, and can handle multiple channels. We have been granted 6 U.S. patents on the approach (with two additional patents pending). Thus, the technology readiness level is 5. On-going development includes a graphical user interface, more robust software, and implementation on a hand-held device (e.g., personal digital assistant). We expect to complete these improvements in 2004, which will allow qualification for a technology readiness level of 6.

Success for such diverse applications suggests that the method can reliably measure condition change in many nonlinear systems. Examples of such new potential applications include combat readiness of soldiers, new complex combat systems, and next-generation system-of-systems (e.g., unit-of-action/future combat systems).

5. ACKNOWLEDGMENTS

We gratefully acknowledge partial support from the U.S. Department of Energy's Materials Science and Engineering Program of the Office of Basic Energy Sciences and from the Nuclear Energy Research Initiative (project# NERI2000-109); from Laboratory Directed Research and Development Program at Oak Ridge National Laboratory, which is managed by UT-Battelle, LLC, for the USDOE under Contract No. DE-AC05-00OR22725; from ViaSys Healthcare Inc. (formerly Nicolet Biomedical Inc. of Madison, WI), which provided human brain wave data under Cooperative Research and Development Agreement #99-0559; and from Physio-Control Corp., which supplied human heart wave data under Cooperative Research and Development Agreement #95-0353.

REFERENCE

L.M. Hively and V.A. Protopopescu, "Detection of Changing Dynamics in Physiological Time Series," *Proc. Nucl. Math. & Comput. Sci.* (Gatlinburg, TN, 6-11 April 2003) Amer. Nucl. Soc., LaGrange Park, IL (2003), paper #117, pages 1-17; reprints are available at http://computing.ornl.gov/cse_home/staff/hively.shtml

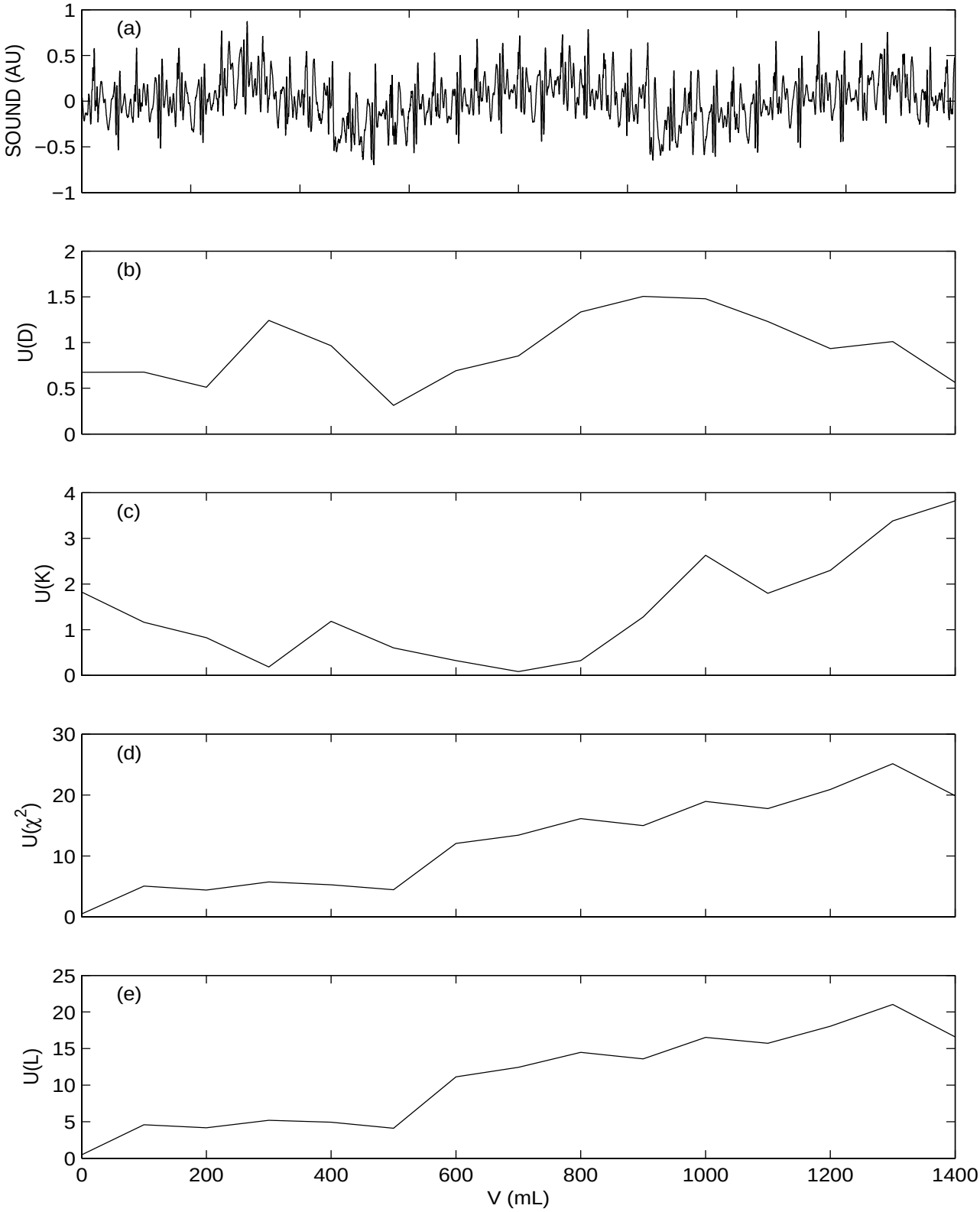

Figure 5: Results from dataset #PTX5, showing time-serial plots for: (a) 4 seconds of raw lung sounds data collected at 10 kHz, (b) correlation dimension, *D,* (c) Kolmogorov entropy, *K*, (d) $U(\chi^2)$, and (e) $U(L)$. The phase-space dissimilarity measures in subplots (d) and (e) are for $d = 3$, $S = 30$, $\lambda = 20$, after removal of breathing artifacts. Each cutest has $N =$ 50,000 points (5 seconds of data).